

Numerical Modelling and Investigation of Longitudinal Flow Turbine Blades for Marine Applications

1.Kadali Sai Durga Prasad, 2.P.S Nagendra, 3.Duddu Hemanth Kumar

Department of Marine Engineering,
Andhra University,
Visakhapatnam , AP, INDIA.

ABSTRACT:

This paper investigates the structural behavior of an 8-meter rotor blade designed for a 1-megawatt floating tidal turbine developed by ÉireComposites Teo. Researchers at the National University of Ireland Galway (NUIG) evaluated the blade's performance under simulated mechanical loads within their Large Structures Research Laboratory.

A crucial aspect of this study involved creating a digital replica (or "digital twin") of the rotor blade using finite element (FE) modeling software like ANSYS. This digital twin utilized layered shell elements to represent the blade's structure.

The research team then validated the accuracy of this digital twin by simulating the blade's response under its design load conditions. This simulation yielded a tip deflection value that differed by only 3% from the actual deflection measured during physical testing in the laboratory.

These results achieve two key goals:

1.Structural Integrity Confirmation: The close match between simulated and measured deflections confirms that the actual blade can withstand the maximum design loads it might encounter during operation.

2.Digital Twin Validation: The small discrepancy between simulation and test data demonstrates the high accuracy of the developed digital twin. This validated digital twin can be used for future analyses and optimizations of the blade design.

Keywords: Tidal Turbine; Ocean Energy; Turbine Rotor Blade; Digital Twin; Experimental Testing; Marine Engineering.

INTRODUCTION

Tidal Energy: A Growing Renewable Source

Renewable energy sources, such as tidal power, have seen rapid growth in recent decades as alternatives to fossil fuels. Tidal energy, harnessed from the predictable ebb and flow of ocean tides, offers a reliable and sustainable power source. Despite the global disruptions caused by the COVID-19 pandemic, the deployment of tidal stream technology in Europe continued to expand, accounting for a significant portion of the worldwide total.

Challenges in Tidal Turbine Blade Design:

While tidal energy holds great promise, its development, particularly in the realm of tidal turbine blades, still lags behind that of wind turbines. Commercial confidentiality and limited availability of test data have hindered progress.

Tidal turbines face unique challenges due to the high density of water compared to air. This dense medium subjects turbine blades to complex loading conditions, necessitating advanced design and performance validation methods. Static testing plays a crucial role in ensuring the structural integrity of these blades under extreme tidal loads.

Ongoing Research and Development:

To accelerate the commercialization of tidal energy, various projects, such as MeyGen, SABELLA, and FloTEC, have been undertaken. These initiatives focus on developing innovative tidal turbine technologies and improving the understanding of their performance. By addressing the challenges associated with blade design and testing, the tidal energy industry can make significant strides towards a more sustainable and resilient energy future.

FE Analysis: A Tool for Tidal Turbine Blade Design

Finite element (FE) analysis is a widely used technique for predicting the stiffness, strength, and fatigue life of tidal turbine blades. Layered shell elements, commonly employed in wind turbine blade modeling, have also been applied to tidal turbine blade design due to their structural similarities. However, the lack of experimental data has limited the validation of these FE models for tidal turbines.

Experimental Validation of Tidal Turbine Blade FE Model:

This paper presents a comprehensive study of a 1 MW tidal turbine blade, one of the largest in the world. The study combines experimental testing and numerical analysis to evaluate the blade's structural behavior and validate the accuracy of its FE model.

The paper provides detailed information on the blade's structural design and the testing program conducted. This program included natural frequency tests and static tests to assess the blade's dynamic and static response.

A FE model was developed to predict the blade's structural behavior under various loading conditions. By comparing the numerical results from the FE model with the experimental data, the paper evaluates the model's accuracy and its ability to accurately predict the blade's performance under design loads.

METHODOLOGY

Blade Description:

Tidal Turbine Blade Design and Manufacturing

The 8-meter tidal turbine rotor blade studied in this research was designed for a floating tidal energy conversion device developed by Orbital Marine Power (OMP). The device features two 1-megawatt tidal turbines, each with a 20-meter rotor diameter.

The tidal blade comprises three main sections: the main body, trailing edge fairings, and tip. The main body, as depicted in Figure 1, was manufactured by ÉireComposites using glass fiber reinforced powder epoxy composite material. This material utilizes ÉireComposites' proprietary Composites Powder Epoxy Technology (CPET).

Compared to conventional glass fiber reinforced polymer (GFRP), CPET-based GFRP offers several advantages, including reduced through-thickness wet-out requirements, precise control of fiber volume fraction, and lower exothermic heat generation during curing. Additionally, the powder epoxy resin used in CPET can be stored at ambient temperatures, extending its shelf life compared to traditional epoxy resins.

The material properties employed in the manufacturing process of the blade are essential for ensuring its structural integrity and performance. These properties include:

Fiber properties: Tensile strength, modulus, and density of the glass fibers.

Matrix properties: Tensile strength, modulus, and density of the powder epoxy resin.

Fiber volume fraction: The percentage of fiber content within the composite material.

Void content: The amount of empty space or voids within the composite.

Cure conditions: Temperature and time required for the epoxy resin to fully cure.

By understanding these material properties, engineers can optimize the blade's design and manufacturing process to achieve the desired performance characteristics.

¹ MeyGen | Tidal Projects, SIMEC Atlantis Energy. <http://simecatlantis.com/projects/meygen/>, accessed 04/2021.

² SABELLA's tidal turbines: tidal stream power to trigger the energy transition. <https://www.sabella.bzh/en/>, accessed 04/2021.

³ FloTEC: Innovation and Networks Executive Agency - European Commission. <https://ec.europa.eu/inea/en/horizon-2020/projects/h2020-energy/ocean/flotec>, accessed 04/2021

Figure 1. The main body of the tidal turbine blade (manufactured at ÉireComposites).



Table 1. Material properties.

	<u>UD</u>	<u>BX</u>	<u>unit</u>
Density	1900	1900	kg/m ³
E1	38805	25944	MPa
E2	12785	25944	MPa
E3	12785	25944	MPa
G12	3670	3570	MPa
G13	3670	3570	MPa
G23	3670	3570	MPa
n12	0.26	0.1289	-
n13	0.26	0.1289	-
<u>n23</u>	<u>0.26</u>	<u>0.1289</u>	<u>-</u>

Blade Structural Composition

Based on the manufacturer's provided structural details, the external surface of the tidal turbine blade can be categorized into three primary components:

- 1. Spar Cap:** The top and bottom structural elements that provide longitudinal strength.
- 2. Leading Panel:** The front section of the blade that faces the oncoming tidal flow.
- 3. Trailing Panel:** The rear section of the blade that follows the tidal flow.

Internally, the main body features a web that extends from approximately 1 meter from the blade's root to its tip. This web connects the upper and lower spar caps, forming an I-beam-like structure that serves as the primary support component of the blade.

Blade Layer Thickness Distribution

The thickness of the blade's various layers, including the spar caps, leading panel, trailing panel, and web, is crucial for ensuring its structural integrity and performance. The distribution of these thicknesses throughout the blade's length can vary based on design considerations and load requirements.

Understanding the layer thickness distribution is essential for accurately modeling the blade's structural behavior using FE analysis and for evaluating its performance under different operating conditions are shown in [The UD presents a layer with a number of uni-directional laminates.](#)

[The BX presents a layer with a number of woven laminates.](#)

[The UD3-BX presents a layer constructed by 25% of woven laminates and 75% of uni-directional laminates. The BX-UD2 presents a layer constructed by 33.3% of woven laminates and 66.7% of uni-directional laminates.](#)

Blade Layup and Thickness Distribution:

This section details the thickness distribution and composition of the blade's various layers, normalized by the maximum thickness for easier comparison.

UD: Represents a layer composed entirely of unidirectional laminates, where fibers run parallel to the primary load direction.

BX: Represents a layer composed entirely of woven laminates, where fibers are interwoven in a fabric-like pattern.

UD3-BX: Represents a hybrid layer containing 75% unidirectional laminates and 25% woven laminates.

BX-UD2: Represents a hybrid layer containing 66.7% unidirectional laminates and 33.3% woven laminates.

Circular Root Design:

The blade's root section is designed with a circular cross-section for optimal connection to the turbine's pitch bearing via 48 steel inserts. This region is crucial as it needs to withstand the significant bending moments generated by the tidal current.

Spar Cap Reinforcement:

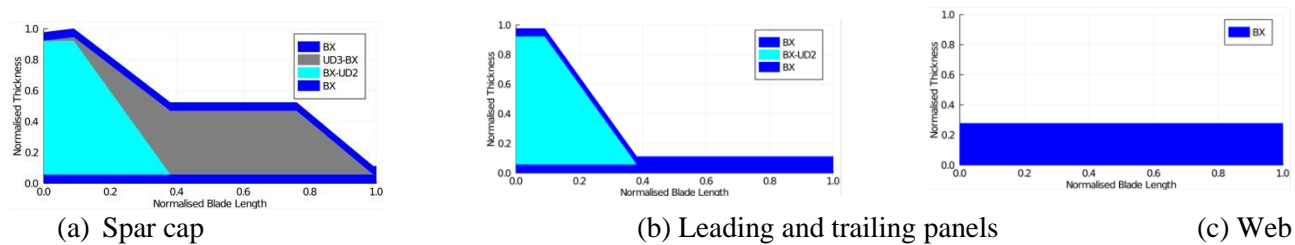
Compared to the leading and trailing panels, the spar cap features an additional BX-UD3 layer situated between the internal and external covers. This enhanced layup strengthens the spar cap, increasing its resistance to flapwise bending loads acting perpendicular to the blade's length.

Material Selection and Shell Thickness:

This design utilizes a GFRP material thick enough to prevent local buckling failures within the blade shell. This differs from wind turbine blades, where lightweight core materials are often used to increase shell thickness without adding significant weight. By relying solely on the GFRP composite, the tidal turbine blade achieves the necessary strength to endure the demanding underwater environment.

Key Takeaways:

- ❖ The blade's thickness varies across its length and is tailored based on the expected loads at different locations.
- ❖ Hybrid laminates combining unidirectional and woven fibers offer a balance of strength and flexibility.
- ❖ The circular root design ensures efficient load transfer from the blade to the turbine via the pitch bearing.
- ❖ The reinforced spar cap enhances resistance to flapwise bending moments.
- ❖ The thick GFRP shell eliminates the need for lightweight core materials, crucial for withstanding underwater loads.



The UD presents a layer with a number of uni-directional laminates.

The BX presents a layer with a number of woven laminates.

The UD3-BX presents a layer constructed by 25% of woven laminates and 75% of uni-directional laminates.

The BX-UD2 presents a layer constructed by 33.3% of woven laminates and 66.7% of uni-directional laminates.

Figure 2. Summary of the layup details of the tidal turbine blade.

Experimental Testing:

Experimental Testing of Tidal Turbine Blade:

A series of structural performance tests were conducted on the tidal turbine blade at the Large Structures Testing Laboratory at NUI Galway. This paper focuses on the natural frequency and static tests conducted during the experimental program.

Test Setup Configuration: As illustrated in Figure 3, the blade's main body was securely mounted to a root support frame designed to withstand the anticipated loads during static testing. The connection between the blade and the support frame was established using 48 steel inserts at a pitch angle of 6 degrees. The blade's pressure side was oriented upwards. The support frame itself was anchored to a reinforced concrete reaction floor to ensure stability during the tests.

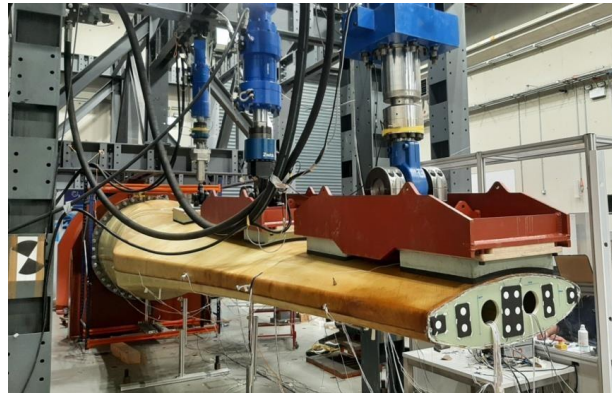


Figure 3. Blade test setup.

Dynamic Characterization: Natural Frequency Tests:

Natural frequency tests were conducted to evaluate the dynamic characteristics of the tidal turbine blade. These tests aimed to identify the inherent vibrational frequencies of the blade in various modes.

Test Instrumentation:

Accelerometers: Five single-axis accelerometers were installed along the pressure side of the blade, and three were placed on the leading edge. These instruments captured the blade's vibration responses during testing.

Excitation Method:

A hammer impact was utilized to excite the blade and induce transient vibrations. This impact was applied to the tip of the blade.

Modes of Interest:

The primary focus of the tests was on the following three vibration modes:

First two flapwise modes: These modes involve the blade bending up and down perpendicular to its plane of rotation (flapwise direction).

First edgewise mode: This mode signifies the blade bending sideways along its leading edge.

First torsional mode: This mode describes the blade twisting about its longitudinal axis.

Impact Direction and Data Acquisition:

To isolate and identify each mode, the impact force was applied in specific directions:

Flapwise and torsional modes: The impact force was directed in the flapwise direction (perpendicular to the blade's plane).

Edgewise mode: The impact force was applied in the edgewise direction (along the leading edge).

The natural frequencies of the blade in each mode were determined using Fast Fourier transform (FFT) analysis of the accelerometer data. To ensure accuracy, each test was replicated three times, and the average values were used for further analysis.

Objective: To validate the structural integrity of the tidal turbine rotor blade under design load conditions.

Standards and Methodology: The testing adhered to the DNVGL-ST-0164 code (DNV, 2015) and IEC TS 61400-23 standards (IEC, 2014). Load application was achieved using three servo-hydraulic actuators mounted on a reaction frame at specific distances from the blade root.

Load Distribution: To accurately simulate design loads, a load distribution system was employed. Actuator 1 applied load directly to the blade surface via a contact pad. For actuators 2 and 3, steel load introduction devices were used to split the applied load equally. These devices, connected to the actuators via swivels, distributed the load to two contact pads each. This mechanism ensured that the testing loads were distributed to five contact areas on the blade, effectively representing the design load distribution.

Conclusion: By following this methodology, the static testing successfully evaluated the blade's ability to withstand the design loads, thereby ensuring its structural reliability for tidal turbine applications.

Load Case Scenarios: The static testing encompassed eight load cases, progressively increasing the applied loads to the maximum design values. The specific loads for each test are detailed in Table 2.

Load Orientation and Pitch Angle: The loads were applied in a downward direction to the blade, which was installed at a pitch angle of 6 degrees. This configuration allowed for the decomposition of the applied actuator loads into flapwise and edgewise components.

Load Calibration and Prioritization: As edgewise extreme loads were deemed non-critical for the blade design, actuator loads were calibrated to precisely match the flapwise design loads. This calibration resulted in approximately 50% of the edgewise design loads being achieved. Torsional extreme loads were also excluded from the test campaign due to their non-critical nature for the blade design.

Table 2. Static load cases and the corresponding actuator loads.

	Actuator 1 [kN]	Actuator 2 [kN]	Actuator 3 [kN]
Load Case 12.5%	19	61	45
Load Case 25%	39	123	90
Load Case 37.5%	58	184	135
Load Case 50%	78	245	180
Load Case 62.5%	97	306	225
Load Case 75%	116	368	270
Load Case 87.5%	136	429	315
Load Case 100%	155	490	360

Instrumentation: To capture the blade's response under various load cases, a comprehensive instrumentation setup was utilized. This included:

Displacement Transducers: Linear Variable Differential Transformers (LVDTs) and linear potentiometers (both with 0.1% linearity) were strategically placed at 3.28 m, 5.13 m, and 7.94 m from the blade root to measure deflections.

Strain Gauges: Electrical resistance strain gauges (with 1% gauge factor uncertainty) were installed at six cross-sections along the blade (0.5 m, 2.16 m, 3.96 m, 5.13 m, 6.16 m, and 7.19 m from the root). These gauges were strategically positioned to monitor strain development on the blade surface (refer to Figure 4 for typical locations).

Support Frame Instrumentation: Additional LVDTs and strain gauges were mounted on the support frame to track blade root rotation and ensure the frame's structural integrity prior to any potential blade failure.

Data Acquisition: This instrumentation enabled the acquisition of valuable data on blade deflections and strain distributions, providing insights into the blade's structural behavior under different loading conditions.

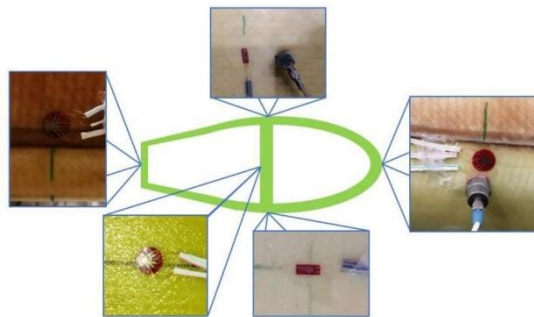


Figure 4. Typical instrumentation at a cross section of the blade, including linear and rosette electrical resistance strain gauges (linear gauges top and bottom photos; rosette gauges left and bottom-left photos) and accelerometers (top and right photos).

Numerical Modelling:

Software and Element Type: The finite element (FE) model of the tidal turbine blade was developed using ANSYS® Academic Research Mechanical, Release 17.1. The blade model employed the SHELL181 element, a four-node shell element with six degrees of freedom per node. To accurately represent the blade's layered structure, multiple layers (with three integration points each) were assigned to each shell element.

Mesh Generation and Contact Regions: The FE model was meshed to simulate the static testing conditions (refer to Figure [Image of meshed FE model]). Nodes anticipated to be in contact with the load pads were specifically selected (highlighted in Figure [Image of highlighted contact nodes]). The applied loads on each pad were calculated and evenly distributed to these selected nodes.

Connection Assumptions and Simplifications: To simplify the model, the connections between the blade's upper half, lower half, and web were assumed to be sufficiently strong to resist the applied loads. Consequently, the connection details were neglected, and the blade was modeled as an integrated component.

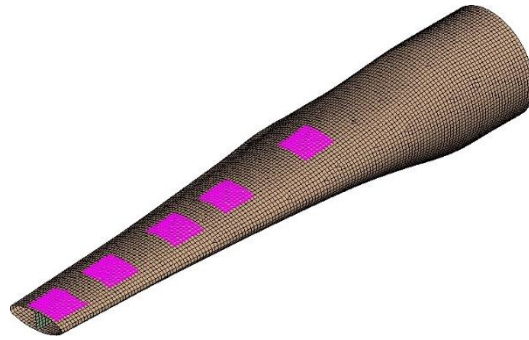


Figure 5. FE model generated in Ansys® Academic Research Mechanical, Release 17.1 (ANSYS, 2016).

RESULTS AND DISCUSSION:

Natural Frequencies:

Comparison of Test and FE Results: A comparison between the natural frequency values obtained from testing and those predicted by the FE model reveals a significant discrepancy. The first three predicted frequencies were found to be over 40% higher than the test results, while the predicted first torsional frequency was 15% lower than the test value. Moreover, the FE analysis failed to capture the second edgewise mode.

Potential Reasons for Discrepancies: Two primary factors could contribute to these inaccuracies:

1. Mass Discrepancy: The FE model's weight (3,820 kg) was underestimated compared to the blade's actual weight (over 4,000 kg). The omission of 48 steel inserts and additional prepreg materials used for connecting the blade halves and web led to this mass discrepancy.

2. Support Frame Flexibility: The values presented in the table represent the natural frequencies of the entire testing system, including the support frame. The flexibility introduced by the support frame could have influenced the system's natural frequencies, resulting in inaccurate predictions from the FE model.

Table 3. Natural frequencies from the test and from the FE analysis.

Mode	Test Frequency [Hz]	FE Frequency [Hz]
1st Flapwise	15.28	21.99
1st Edgewise	17.81	26.36
2nd Flapwise	31.34	54.79
2nd Edgewise	31.48	NA
1st Torsional	84.51	71.66

Static Testing:

Blade Structural Integrity and Deflection Behavior under Varying Loads

To assess the blade's structural performance under various loading conditions, eight load cases were analyzed. Due to consistent behavior across these cases, four representative load cases (25%, 50%, 75%, and 100% of design load) were selected for detailed analysis and result presentation.

Under the maximum design load (100%), the blade exhibited no signs of failure or cracking, confirming its structural integrity. Static loading resulted in a slight root rotation, primarily influenced by the root moment (5714 kNm). This rotation was measured using LVDTs installed on the support frame. For the 100% load case, a root rotation of 0.17° was observed.

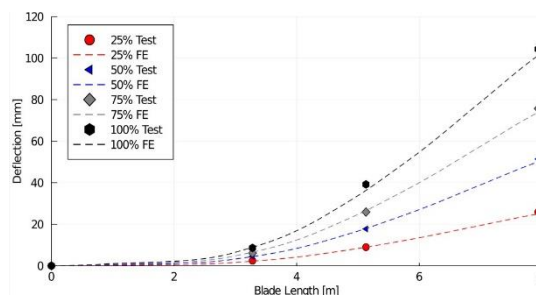
Considering the blade's 8-meter length, this rotation led to an additional tip deflection of approximately 23 mm. To account for this effect, the deflection data from the three displacement transducers were adjusted based on the root rotation angle. Figure 6 summarizes the blade deflections under all four load cases.

The maximum blade tip deflection was found to be 104 mm, representing 1.3% of the blade length. This result indicates that the tidal turbine blade possesses satisfactory stiffness, demonstrating its ability to withstand the intended loads without excessive deformation.

Figure 6 presents a comparison between the predicted blade deflections from the digital twin and the corresponding experimental data obtained from physical laboratory tests. Across all four load cases, the numerical results demonstrated excellent agreement with the experimental measurements.

Under the 100% design load, the predicted tip deflection was approximately 101 mm, which is 3% lower than the experimental value. This slight discrepancy suggests that the FE model, while accurately predicting the overall stiffness of the tidal turbine rotor blade, may be marginally conservative in its deflection estimates.

The observed underestimation of deflections in the FE analysis for all four load cases indicates that the stiffness of the model is slightly higher than that determined through physical testing. This finding highlights the potential need for further refinement of the material properties or structural assumptions used in the FE model to achieve



even closer alignment with experimental observations.

Figure 6. Deflection comparisons between the testing data and FE results.

Figure 7 presents the normalized longitudinal strain along the spar cap, leading edge, and trailing edge of the blade for the four selected load cases. The strain values are normalized based on their maximum absolute values, with the longitudinal direction defined as extending from the root to the tip.

The maximum absolute strain of 0.002 was observed on the pressure side of the spar cap under the 100% load case. Given the strain limit of the BX GFRP material (± 0.025), this indicates that no material failure occurred under the maximum design loads.

The FE-predicted strain values are compared with experimental data in Figure 7. For strains along the spar caps on both the pressure and suction sides, the FE model demonstrated good agreement with the strain gauge measurements. However, the predicted values were generally slightly lower than the experimental data, suggesting that the FE model may have slightly overestimated the blade stiffness. This finding aligns with the observations made during the deflection comparisons.

Significant differences were observed between the numerical and experimental strain results along the leading and trailing edges of the blade. These discrepancies can be attributed to the connection details. As described in Section 2.1, the upper and lower halves of the blade main body were joined using prepregs along the leading and trailing edges. This connection detail was not explicitly represented in the numerical model.

The simplification of the connection details in the FE model may have contributed to inaccurate strain predictions in the numerical analysis. This observation aligns with the findings of Peeters et al. (2019), who highlighted that shell element wind turbine FE models, while capable of accurately predicting deflections, may struggle to simulate the stress and strain distribution within the connection region.

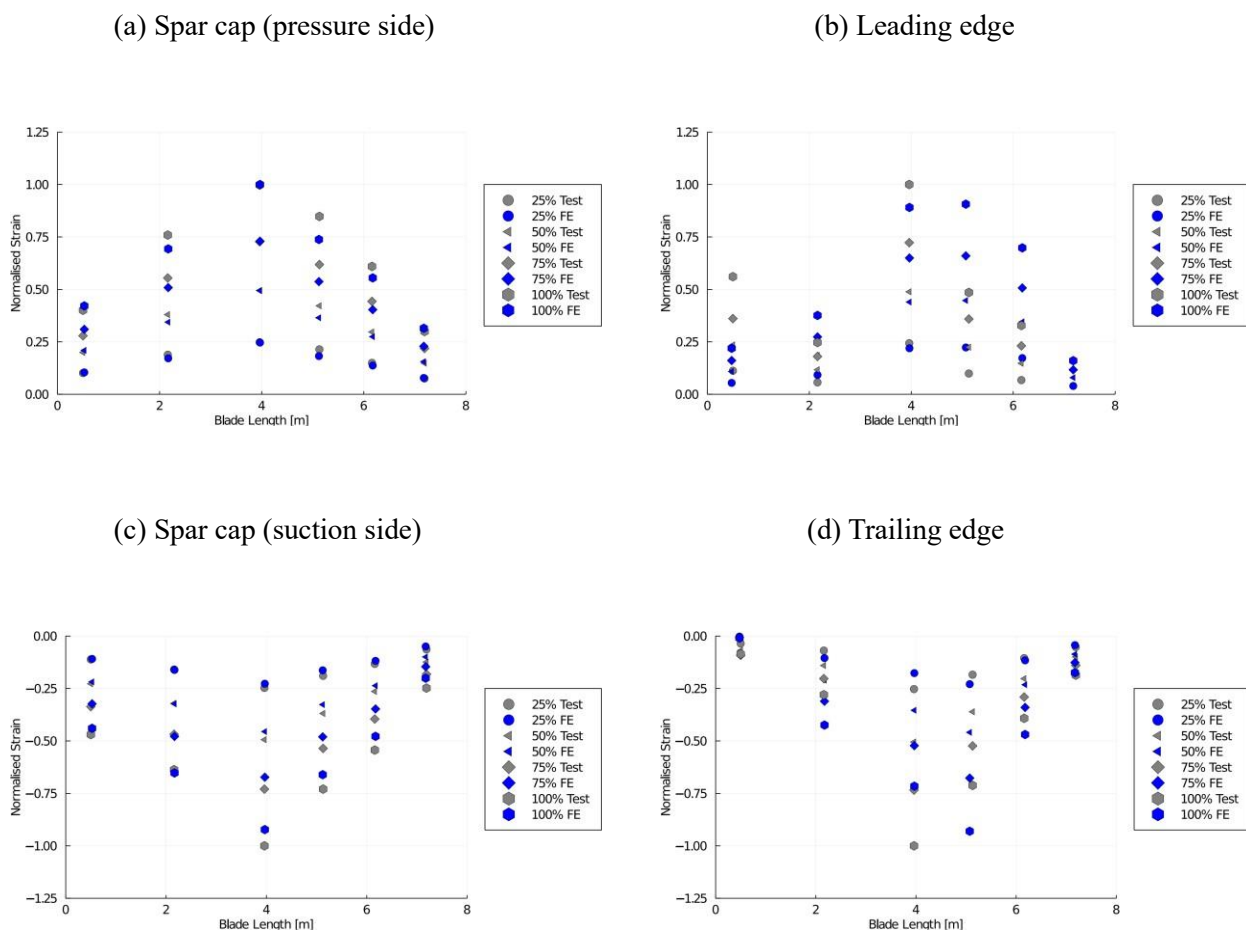


Figure 7. Normalised longitudinal direction strain comparisons along the length of the blade between the testing data and FE results.

CONCLUSIONS:

This paper presents a comprehensive study of the structural behavior of a 1 MW tidal turbine rotor blade. A series of experimental tests were conducted in conjunction with the development of a layered shell element FE model, which was based on the blade design details and testing program.

The results from both the physical testing and digital twin analysis allowed for a thorough evaluation of the blade's performance under design loads and the accuracy of the FE model. The following conclusions can be drawn:

Static testing demonstrated that the tidal turbine blade is capable of withstanding the maximum design loads without experiencing any failures or cracks. This outcome validates the blade's structural integrity and ensures its safety under extreme load conditions.

The developed shell element model, serving as the digital twin, demonstrated accurate predictions of blade deflection under testing loads. Additionally, the model effectively captured strain values on the spar cap, indicating its suitability for modeling tidal turbine blades. Given that the spar caps are the primary load-bearing structures of the blade, the shell element approach is well-suited for analyzing their structural behavior.

Despite its overall accuracy, the digital twin exhibited limitations in predicting the natural frequencies and strain data along the leading and trailing edges. These discrepancies can be attributed to the simplification of connection details in the model, highlighting the need for more refined representations of these critical regions for improved accuracy.

In future iterations of the FE model, the connection details of the blade will be incorporated to enhance the accuracy of stress and strain predictions. By leveraging these refined numerical results, fatigue analysis will be conducted to ensure the blade's structural integrity and compliance with the required 20-year operational lifespan.

REFERENCES

- Ansys® Academic Research Mechanical, Release 17.1 Help System. (2016). *Mechanical Application Documentation*, ANSYS, Inc.
- DNV. (2015). *Standard DNVGL-ST-0164 Tidal turbines*. Det Norske Veritas (2015).
- Fagan, E.M., Kennedy, C.R., Leen, S.B. and Goggins, J. (2016). Damage mechanics based design methodology for tidal current turbine composite blades. *Renewable Energy*, 97, 358-372.
- Fagan, E.M., Flanagan, M., Leen, S.B., Doyle, A. and Goggins, J. (2017). Physical experimental static testing and structural design optimisation for a composite wind turbine blade. *Composite Structures*, 164, 90-103.
- Fagan, E.M., De La Torre, O., Leen, S.B. and Goggins, J. (2018) Validation of the multi-objective structural optimisation of a composite wind turbine blade. *Composite Structures*, 204, 567-577.
- Fagan, E.M., Wallace, F., Jiang, Y., Kazemi, A. and Goggins, J. (2019). Design and testing of a full-scale 2 MW tidal turbine blade. *Proceedings of the Thirteenth European Wave and Tidal Energy Conference*, Napoli, Italy.
- IEA. (2020). *World Energy Outlook 2020*. International Energy Agency, Paris, France.
- IEC. (2014). *IEC 61400-23: 2014: Wind turbine generator systems—part 23: full-scale structural testing of rotor blades*. International Electrotechnical Commission, Geneva, Switzerland.
- Jiang, Y., Fagan, E.M. and Goggins, J. (2019). Structural design and optimisation of a full-scale tidal turbine blade. *Proceedings of the Thirteenth European Wave and Tidal Energy Conference*, Napoli, Italy.

Murray, R.E., Nevalainen, T., Gracie-Orr, K., Doman, D. and Pegg, M.J. (2016). Passively adaptive tidal turbine blades: Design tool development and initial verification. *International Journal of Marine Energy*, 14, 101-124.

OEE. (2021). *Ocean Energy - Key trends and statistics 2020*. Ocean Energy Europe, Brussels, Belgium. OEE. (2020). *2030 Ocean Energy Vision*. Ocean Energy Europe, Brussels, Belgium.

Peeters, M., Santo, G., Degroote, J. and Van, P.W (2019). Comparison of Shell and Solid Finite Element Models for the Static Certification Tests of a 43 m Wind Turbine Blade. *Energies*, 11, 1346.

Wang, L., Kolios, A., Nishino, T., Delafin, P. and Bird, T. (2016). Structural optimisation of vertical-axis wind turbine composite blades based on finite element analysis and genetic algorithm. *Composite Structures*, 153, 123-138.